https://doi.org/10.5194/cp-2020-23
Preprint. Discussion started: 5 March 2020

Climate of the Past Discussions

Sea surface temperature in the Indian sector of the Southern Ocean over the Late Glacial and Holocene

Lisa C. Orme[1,2], Xavier Crosta[3], Arto Miettinen[1,4], Dmitry V. Divine[1,5], Katrine Husum[1], Elisabeth Isaksson[1], Lukas Wacker[6], Rahul Mohan[7], Olivier Ther[3], Minoru Ikehara[8]

[1]Norwegian Polar Institute, Tromsø, 9296, Norway
[2]ICARUS, Department of Geography, Maynooth University, Maynooth, Ireland
[3]UMR 5805 EPOC, Université de Bordeaux, Bordeaux, France
[4]Faculty of Biological and Environmental Sciences, University of Helsinki, Helsinki, 00014, Finland
[5]Department of Mathematics and Statistics, The Arctic University of Norway, 9037, Tromsø, Norway
[6]Department of Physics, ETH Zürich, 8093 Zürich, Switzerland
[7]National Centre for Polar and Ocean Research, Ministry of Earth Sciences, Government of India, Vasco-da-Gama, Goa 403 804, India
[8]Center for Advanced Marine Core Research, Kochi University, Nankoku, 783-8502, Japan

Correspondence to: Lisa C. Orme (lisa.orme@mu.ie)

Abstract. Centennial and millennial scale variability of Southern Ocean temperature is poorly known, due to both short instrumental records and sparsely distributed high-resolution temperature reconstructions, with evidence for past temperature variability instead coming mainly from ice core records. Here we present a high-resolution (~60 year), diatom-based sea-surface temperature (SST) reconstruction from the western Indian sector of the Southern Ocean that spans the interval 14.2 to 1.0 ka BP (calibrated kiloyears before present). During the late deglaciation, the new SST record shows cool temperatures at 14.2-12.9 ka BP and gradual warming between 12.9-11.6 ka BP in phase with atmospheric temperature evolution. This supports that the temperature of the Southern Ocean during the deglaciation was linked with a complex combination of processes and drivers associated with reorganisations of atmospheric and oceanic circulation patterns. Specifically, we suggest that Southern Ocean surface warming coincided, within the dating uncertainties, with the reconstructed slowdown of the Atlantic Meridional Overturning Circulation (AMOC), rising atmospheric CO_2 levels, changes in the southern westerly winds and enhanced upwelling. During the Holocene the record shows warm and stable temperatures from 11.6-8.7 ka BP followed by a slight cooling and greater variability from 8.7 to 1 ka BP, with a quasi-periodic variability of 200-260 years as identified by spectral analysis. We suggest that the increased variability during the mid to late Holocene may reflect the establishment of centennial variability in SST connected with changes in the high latitude atmospheric circulation and Southern Ocean convection, as identified in models.

1 Introduction

Research into the sequence of events associated with the deglacial period has highlighted that there were contrasting patterns of warming and cooling between the southern and northern high latitudes, considered to have resulted from global-

https://doi.org/10.5194/cp-2020-23
Preprint. Discussion started: 5 March 2020

Climate of the Past Discussions

scale processes, namely fluctuations in the strength of the AMOC and latitudinal shifts in the major atmospheric circulation cells. For example during the Younger Dryas (13.02-11.76 ka BP) a prolonged weakening of the AMOC reduced the northward heat transport in the Atlantic allowing heat to accumulate in the South Atlantic, causing a 'bipolar seesaw' characterised by opposite ocean temperature anomalies between the two hemispheres (Denton et al., 2010 and references therein). These temperature changes caused a rapid alteration of the atmospheric circulation, with a southward shift of the Intertropical Convergence Zone (ITCZ) and Southern Westerly Winds (SWW). A combination of processes including enhanced eddy transport of heat across the Antarctic Circumpolar Current (ACC), upwelling of warm water and dissipation of sea ice then resulted in warming of the Southern Ocean and Antarctica (Levermann et al., 2007; Screen et al., 2009; Denton et al., 2010). Finally, the increased upwelling in the Southern Ocean enhanced CO_2 outgassing and thus warming globally. Despite many of these processes occurring within the Southern Ocean the strongest evidence for the patterns and magnitude of southern high latitude warming during the Younger Dryas comes from Antarctic ice cores (e.g. Stenni et al., 2011). Although a number of records from the Southern Ocean show warming during the Younger Dryas, the timing, magnitude and duration of warming are far from consistent between records (Bianchi and Gersonde, 2004; Divine et al., 2010; Siani et al., 2013; Xiao et al., 2016). This is likely due to variable temporal resolutions and uncertain age constraints of records and regional temperature differences. Acquiring high-resolution proxy records of past sea surface temperature (SST) is therefore important for establishing the spatio-temporal patterns of warming in the Southern Ocean and their link with Antarctic temperature variability.

During the Holocene the majority of records from the open ocean of the Atlantic and Indian sectors of the Southern Ocean show that the early Holocene (~12 to 9 ka BP) was warm with cooler temperatures during the mid to late Holocene (e.g. Bianchi and Gersonde, 2004; Nielsen et al., 2004; Anderson et al., 2009; Xiao et al., 2016). The suggested causes of these temperature changes include variations in southern hemisphere insolation (e.g. Shevenell et al., 2011; Xiao et al., 2016), northern hemisphere insolation (e.g. Nielsen et al., 2004) and weakening of the AMOC in response to northern hemisphere deglaciation (Renssen et al., 2010).

There is also evidence of centennial variability of southern high latitude climate through the Holocene as shown by some palaeoclimate records, including those from the Southern Ocean (e.g. Leventer et al., 1996; Crosta et al., 2007; Katsuki et al., 2012) and those reflecting atmospheric circulation changes such as the Southern Annular Mode (SAM) (e.g. Moreno et al., 2014; Turney et al., 2016). Observational and modelling evidence have suggested that centennial fluctuations in deep convection in the Southern Ocean (Weddell Sea) lead to variability in the surface water temperature of the Southern Ocean and the strength of the atmospheric circulation (Latif et al., 2013). Others have linked the oscillations to AMOC variability (Debret et al., 2009) or solar activity (e.g. Leventer et al., 1996; Crosta et al., 2007; Turney et al., 2016). To understand further how the Southern Ocean temperature has varied during the Holocene there is a need for high-resolution records capturing centennial variations.

We present a diatom-based SST reconstruction from the western Indian sector of the Southern Ocean spanning the last 14.2 thousand years with an average temporal resolution of 60 years. The length and high resolution of the record provides

https://doi.org/10.5194/cp-2020-23
Preprint. Discussion started: 5 March 2020

Climate of the Past Discussions

new information about the patterns, timing and magnitude of temperature variability through the late deglaciation and the Holocene.

2 Study Area

The Conrad Rise is located in the west Indian sector of the Southern Ocean (around 54 °S, 40°E, Figure 1) close to the Atlantic Sector. The rise is <3000 m depth, with two sea mounts (Ob Bank and Lena Seamount) at depths of 300 m (Ansorge et al., 2008). The Conrad Rise is situated within the diatom ooze belt, which circles Antarctica, extending from the Subantarctic Front in the north to the late winter/spring sea ice extent in the south.

Today the site is located within the Permanent Open Ocean Zone (POOZ), with the mean winter sea ice limit lying to the south at 59°S (Park et al., 1998). The mean summer SST at 10 m depth is 3.5°C (World Ocean Atlas, 2013). Summer measurements show that at the Conrad Rise the surface mixed layer extends to 70-80 m depth with temperatures of 2-2.5 °C and salinity of 33.90 – 33.95 psu (Park et al., 1998; Anilkumar et al., 2006). Beneath persists the Winter Water layer, a remnant of the previous winters mixed layer capped by seasonal warm, fresh water, which at the Conrad Rise is estimated to have minimum temperatures (0.5 – 1.5 ºC) at 150-200 m and salinity of 34.05-34.1 psu (Park et al., 1998). The surface oceanographic characteristics are likely influenced by the atmospheric climate and circulation. The core of the SWW has been situated north of the Conrad Rise at approximately 52 °S during the period 1979-2010 AD (Swart and Fyfe, 2012). Across the Southern Ocean positive SAM anomalies cause stronger, southward shifted westerlies, and this also alters SST, causing cooling in the Antarctic Zone due to stronger Ekman transport of cold Antarctic surface water to the north (Lovenduski and Gruber, 2005).

The Conrad Rise is situated within the Antarctic Circumpolar Current (ACC), which consists of several fronts. To the north of the Conrad Rise is a merged front (combined Agulhas Return Front, Southern Subtropical Front and northern Subantarctic Front) at 40-43°S, which has a steep surface temperature range of 10 to 19 °C (Anilkumar et al., 2006) while the southern Subantarctic Front (SAF) lies at approximately 45°S (Sokolov and Rintoul, 2009). The Polar Front is defined by the maximum northern extent of the 2°C isotherm between 100-300 m. Some modelling and observations support that two branches of the Polar Front flow to the north and south of the Conrad Rise, transporting 35 and 25 Sv of water, respectively, with low flow velocities over the rise itself (Pollard and Read, 2001; Ansorge et al., 2008; Sokolov and Rintoul, 2009). However, assessments of the Polar Front position based on identification of a subsurface temperature minima indicate that it is in fact situated to the north, passing between the Conrad Rise and Crozet Islands at approximately 50°S where it varies by season and year over a range <2° latitude (Pauthenet et al., 2018). Topography has a strong influence on the position and form of the ACC in this region. To the west of the Conrad Rise across the Enderby Basin the lack of topographic constraint means that large meanders in the ACC are likely (Pollard and Read, 2001) and variations in the Polar Front position also occur over the flat region to the east of the Conrad Rise (Pauthenet et al., 2018). However, at the Conrad Rise, branches of the Polar Front

https://doi.org/10.5194/cp-2020-23
Preprint. Discussion started: 5 March 2020

become topographically trapped and therefore have low spatial variability through time (Pollard and Read, 2001; Pauthenet et al., 2018).

3 Materials and methods

3.1 Core sampling and sediment description

The 2.48 m long core KH-10-7 COR1GC was retrieved from the Conrad Rise in the southwestern Indian sector of the Southern Ocean (54.2673°S, 39.7663°E, Fig. 1, water depth of 2834 m) using a gravity corer during the expedition KH-10-7 on board the R/V *Hakuho-Maru* in 2010.

The sediment consisted of homogenous diatom ooze; from 2.48 to 2.2m the sediment colour was greenish-grey, while above this the sediment had a pale yellow colour. At approximately 5 cm depth there was a dark grey horizon.

3.2 Age model

Fifteen AMS radiocarbon dates were obtained on mono-specific samples of the planktic foraminifera Neogloboquadrina pachyderma sinistral. The core chronology was constructed in Bacon version 2.3.3. (Blaauw and Christen, 2011), an age-depth modelling technique that uses Bayesian statistics to reconstruct accumulation histories for deposits, by combining radiocarbon and other dates with prior information. This analysis used the Marine13 calibration dataset (Reimer et al., 2013). The shape of sedimentation rate and memory strength parameters used in the Bacon modelling were set to 1.5 and 4, respectively.

To correct the raw radiocarbon ages we used a constant reservoir age of 890 ± 100 years recommended for this region (http://radiocarbon.LDEO.columbia.edu/) (Butzin et al., 2005). The reservoir age may have varied through time, particularly during the deglaciation when ventilation of deep waters occurred. In the Atlantic sector of the Southern Ocean, the comparison of radiocarbon ages and ^{226}Ra decay in barite suggests large variations in regional reservoir ages during the Holocene (van Beek et al., 2002). However, because large variations of ~400 years were observed between consecutive depths, we believe that this method is not reliable. Therefore age reservoir variation during the past 14 ka are unknown for this sector. Fortunately, in the Pacific sector Holocene reservoir ages have been estimated in the Ross Sea through a comparison of ^{14}C and U-Th dating of corals, which showed limited changes in reservoir age during the last 6 ka BP (Hall et al., 2010). In the east Pacific sector (core MD07-3088, Figure 1) a comparison between radiocarbon and tephra dating of marine sediments suggests that at 14 and 11.5 ka BP the reservoir age was 975-920 years, while in the mid-late Holocene it was 800 years (Siani et al., 2013), indicating a change of 100-175 years over our study period. Assuming that the magnitude of changes in reservoir ages were comparable across the Southern Ocean this supports a maximum change in reservoir age of 100 to 200 years through the late deglacial to Holocene transition. Because there were seemingly limited variations in the mean reservoir age over the last 14 ka, and we are

https://doi.org/10.5194/cp-2020-23
Preprint. Discussion started: 5 March 2020


Climate of the Past Discussions

not assessing leads and lags between records, we believe it is more sensible to apply a constant reservoir age correction. We acknowledge that there is greater age uncertainty in the late deglacial section of the COR1GC reconstruction.

3.3 Diatom analysis

Diatom analysis was conducted at ~1 cm intervals. Slide preparation and counting of over 300 diatom valves per sample followed standard methods (Crosta and Koç, 2007). Summer SST and winter sea ice concentration (WSIC) were estimated using the Modern Analogue Technique (MAT) applied to diatom assemblages (Crosta et al., 2004). This method uses a modern database composed of 249 surface sediment samples. Modern summer (January-February-March) SSTs were interpolated on a 1°*1° grid from the World Ocean Atlas 2013 (Locarnini et al., 2013) using Ocean Data View (Schlitzer, 2014). Winter sea ice concentration was interpolated on a 1°*1° grid from the numerical atlas of Schweitzer (1995). The MAT was implemented from the "bioindic" package (Guiot and de Vernal, 2011) built on the R-platform (http://cran.r-project.org/) and used the relative abundances of 32 diatom species and the chord distance to select the five most similar modern analogs. The threshold above which modern analogs are supposed to be too dissimilar to the fossil assemblage is fixed at the first quartile of random distances on the validation/modern dataset. Quantitative estimates of summer SST and WSIC are a similarity-weighted mean of the SST or WSIC associated with the selected modern analogs (Guiot et al., 1993). This method yields a R^2 of 0.96 and a root mean square error of prediction of ~1°C for summer SST and a R^2 of 0.92 and a root mean square error of prediction of ~10% for WSIC.

The total diatom abundance, or the number of diatom valves per gram of dry sediment, was calculated to provide an approximation of the productivity through time following the method described in Crosta et al. (2008). This method allows only an approximation of the surface productivity because the diatom abundance in the sediment can also be affected by factors such as diatom dissolution during settling and deposition, lateral transport within the water column or at the water-sediment interface, and variable dilution by lithogenic particles.

3.4 SiZer analysis

SiZer (Significance of Zero Crossings of the Derivative) (Chaudhuri and Marron, 1999) is a scale-space technique that was applied to explore statistically significant features in the reconstructed SST. A key idea in SiZer is that significant features are found at different time scales, that is, at different levels of data smoothing. This makes it particularly useful in paleoclimate studies since the salient features in a timeseries may depend heavily on the time horizon on which it is analysed. This method has been used previously in a number of palaeoclimate studies (e.g. Berner et al., 2008).

In SiZer the observed data are viewed at varying levels of resolution while the notion of scale is controlled through the bandwidth h in the local linear kernel estimator. For each scale h and time t of the signal, a test is performed to see whether the smoothed data series has a local derivative significantly different from zero, in other words, to see if the slope at a specific time point for a given scale is significantly different from zero. The Gaussian kernel estimator embedded in SiZer does not

https://doi.org/10.5194/cp-2020-23
Preprint. Discussion started: 5 March 2020


Climate of the Past Discussions

require an analysed timeseries to be evenly spaced, the method is therefore applied to the data directly without any prior resampling. SiZer visualises the output of the analysis in a feature map where the results are displayed as a function of time and scale.

3.5 Spectral analysis

Many geophysical time series have distinctive red noise characteristics that can be modelled by a first order autoregressive (AR1) process. REDFIT spectral analysis (Schulz and Mudelsee, 2002) was carried out on the Holocene section of the SST reconstruction to establish whether quasi-periodic variability existed. This method of spectral analysis was selected as it has been designed for unevenly spaced paleoclimate data, therefore avoiding the need to resample and interpolate the data, which can introduce bias (Schulz and Mudelsee, 2002). The analysis was conducted using the REDFIT tool integrated in the PAST 3.25 software (Hammer et al., 2001) using window = Welch, segments = 2 and oversampling = 2. The tau value was 27.46. The appropriateness of the AR1 model to describe the analysed data was tested using a nonparametric runs test (Bendat and Piersol, 1986) embedded in the package.

4 Results

The core covers the period from 14.2-1 ka BP and has a mean sedimentation rate of ~20 cm ka^{-1} (Table 1; Figure 2). The sedimentation rate decreased from 14 to 12 ka BP when it stabilised at its lowest values until 10 ka BP. It subsequently increased over the course of the Holocene to reach values >20 cm ka-1 during the late Holocene.

The diatom assemblage of COR1GC is dominated by pelagic open ocean taxa, particularly *Fragilariopsis kerguelensis* and *Thalassiosira lentiginosa*, with accompanying species typical of the Polar Front Zone (PFZ) and POOZ (Figure 3). PFZ (*F. kerguelensis*, *Thalassionema nitzschioides var lanceolata*) and Subantarctic Zone (SAZ) (*Thalassiosira oestrupi*) species, were more abundant in the interval 12-9.5 ka BP, with lowest relative abundances at 14.2-12 ka BP and 4-1 ka BP. Conversely, POOZ species abundances (especially *Thalassiothrix antarctica*, *Thalassiosira gracilis*, *Fragilariopsis separanda* and *Fragilariopsis rhombica*) were lower at 14.2-9.5 ka BP, after which point they gradually increased in proportion over the Holocene. Diatom species associated with sea ice, including *Fragilariopsis ritscheri*, *Fragilariopsis curta*, *Fragilariopsis cylindrus, Porosira glacialis*, *Fragilariopsis obliquecostata* and *Thalassiosira tumida*, had individually low average abundances of <0.3%. These species have been grouped together (Figure 3). The sea ice species were present in low abundances through the record, but were slightly more abundant between 14.2-12.6, 7.6-6.2 and 3.9-1 ka BP and lower from 12.6-7.6 and 6.2-3.9 ka BP.

The estimated total diatom abundance shows a decreasing trend through the record, ranging from abundances of ~1200-600 millions of diatom valves per gram of dry sediment (10^6 dv/g) between 14 and 6 ka BP, ~600 10^6 dv/g at 6-4.2 ka BP and ~300 10^6 dv/g at 4.2-1 ka BP.

https://doi.org/10.5194/cp-2020-23
Preprint. Discussion started: 5 March 2020


Climate of the Past Discussions

The SST reconstruction for COR1GC shows that during the 14.2 - 12.9 ka BP period the average temperature was 2.9 °C (range 1.8-4.1 °C) (Figure 4), which was followed by a phase of warming between 12.9 and 11.6 ka BP when temperatures increased from 2.1 to 5 °C. Between 11.6 and 8.7 ka BP SST's were on average 4.3 °C with minima no lower than 3.3 °C and a standard deviation of 0.4 °C. After 8.7 ka BP the SST record shows a slightly lower average of 3.9 °C, a slight cooling trend, minima of 3-2.2 °C and standard deviation of 0.7 °C. The record shows that during the warmer interval at 11.6-8.7 ka BP the temperature varied less than after 8.7 ka BP, indicating a potentially more stable climate during the early Holocene and a cooler and more variable climate during the mid to late Holocene. SiZer analysis flags three events as statistically significant: the two short-term cooling events at ~8.2 ka BP and ~2.2 ka BP and the warming trend during the deglaciation, the latter of which is marked as significant when identifying variability over a broad range of timescales (Figure 5). Spectral analysis conducted using the REDFIT method shows that during the Holocene there were quasi-periodic oscillations of 220 and 260 years, significant above the 95% false alarm level (Figure 6).

Summer sea ice did not reach the Conrad Rise through the last 14.2 ka BP (reconstruction not shown) and winter sea ice concentrations were very low and below the RMSEP throughout the period (Figure 4). These data however suggest slightly more extensive sea ice cover between 14 and 12 ka BP and after 8 ka BP, and a slight retreat of winter sea ice between 12.2 and 8 ka BP when SSTs were ~1°C higher than today. Relatively low values of the inferred winter sea ice concentration suggest only sporadic and relatively short-term (perhaps decadal to multidecadal scale) expansions of winter sea ice to the coring location throughout the Holocene.

5 Discussion

5.1 Southern high latitude temperature

The millennial trends in the COR1GC temperature record are similar in timing to SST records from the Atlantic sector of the Southern Ocean (Nielsen et al., 2004; Anderson et al., 2009; Xiao et al. 2016; Figure 7 A and B) within the age uncertainty of each record. Many of these show cooler temperatures at ~14.2-12.9 ka BP during the interval known as the Antarctic Cold Reversal (ACR: 14.7-12.7 ka BP; Stenni et al., 2011), gradual warming during the Younger Dryas (or Termination 1b), high temperatures between 11.6 and 8.7 ka BP during the Early Holocene, followed by a cooling trend thereafter. Another SST reconstruction from the Conrad Rise (PS2606-6; Figure 7C; Xiao et al., 2016), with lower temporal resolution than the COR1GC record, shows warm temperatures during the ACR and the early Holocene along with a slight cooling during the Younger Dryas, at odds with the other records from the POOZ. We suggest that the opposite trend in the PS2606-6 record during the late deglaciation is related to chronological issues, as it is the only SST record that is out-of-phase during this period. Although most records, including COR1GC, show a long-term cooling over the Holocene (Xiao et al., 2016), cores located north of the modern APF generally show a late Holocene warming trend (Figure 7; Nielsen et al., 2004; Siani et al., 2013).

https://doi.org/10.5194/cp-2020-23
Preprint. Discussion started: 5 March 2020


Climate of the Past Discussions

The records from the Bouvet Island region and the Conrad Rise (Figure 7 A-D; Xiao et al., 2016) show that the magnitude of warming between the ACR and early Holocene was 1-2°C. Nevertheless, there are variations in the exact magnitudes of the temperature fluctuations between the different records. Some previous records suggested that the SST during the ACR and the mid-late Holocene were similar (Nielsen et al., 2004; Anderson et al., 2009; Xiao et al., 2016; Figure 7 A-C). Our new record from core COR1GC conversely shows SSTs were 1°C lower during the ACR compared to the mid-late Holocene, in agreement with air temperature records (Figure 7E-F).

Indeed, the millennial temperature evolution of the COR1GC record during the deglacial and early Holocene closely resembles the patterns of atmospheric temperature reconstructed from Antarctic ice core water isotope records (Figure 7 E and F; EPICA community members, 2006; Jouzel et al., 2007; Stenni et al 2011). The start of the COR1GC record at 14.2 ka BP is after the beginning of the ACR (at 14.7 ka BP; Stenni et al., 2011) meaning that the timing of the onset of the ACR at the Conrad Rise cannot be established. However despite some degree of dating uncertainty, in part caused by potentially variable reservoir ages, the warming from 12.9 - 11.6 ka BP appears closely aligned with the timing of warming identified in the ice core records at 12.7-11.9 ka BP (Stenni et al., 2011). A good synchronicity between Southern Ocean SST and Antarctic temperature evolution over the deglacial was also shown by a planktic foraminifera-based SST reconstruction from core MD07-3088 from the eastern Pacific sector, which like the COR1GC record showed cold temperatures during the ACR, followed by gradual warming between c.12.7 and 11.5 ka BP and relatively warm conditions through the Holocene (Siani et al., 2013; Haddam et al., 2018). This record was constrained by both radiocarbon dates and tephra horizons minimising dating uncertainties (Siani et al., 2013), which supports the chronological framework of core COR1GC and the new SST record. The warmer early Holocene temperatures that followed at 12-8.7 ka BP are observed widely in ice core, terrestrial and coastal records from across Antarctica (Stenni et al., 2011; Verleyen et al., 2011; Figure 7E and 7F). Together this evidence suggests that the sea surface and atmospheric temperatures across the southern high latitudes varied synchronously during the deglacial to Holocene transition.

5.2 Causes of temperature variability

The SST variations may have been due to a number of factors, including in response to atmospheric temperature changes, variations in the AMOC, changes in the strength and position of the SWW and shifts in the location of the ACC fronts relative to the core site. Here these causes will be discussed in relation to the Younger Dryas and Holocene climate patterns.

5.2.1 Younger Dryas and Termination 1b

Southern high latitude warming (Termination 1b) during the Younger Dryas is widely considered to be the result of a slowdown in the AMOC, which caused reduced northward heat transport and the accumulation of heat in the southern hemisphere (Broecker, 1998; Stocker and Johnsen, 2003). This is supported by a close agreement between the timing of warming in the COR1GC and ice core records with reconstructed AMOC weakening (McManus et al., 2004; Figure 8A). The

https://doi.org/10.5194/cp-2020-23
Preprint. Discussion started: 5 March 2020


Climate of the Past Discussions
Open Access
EGU

AMOC weakening between 12.8-11.7 ka BP is thought to have caused a reduced northward heat transport, cooling of the North Atlantic and warming of the South Atlantic, which caused the ITCZ to be positioned further south (Figure 8B; Hughen et al., 1996). It is considered that this in turn caused poleward-shifted and strengthened SWW (Denton et al., 2010; Pedro et al., 2018). Evidence from the Southern Ocean supports that the SWW were stronger over a longer interval from 14 to 11 ka BP but only shifted southwards to a more poleward position at 12.5 ka BP (Fig 8C; Fletcher and Moreno, 2011; Saunders et al., 2018).

The changes to the SWW during Termination 1b are thought to have warmed the Southern Ocean in a number of ways, including through the southward migration of the Polar Front, causing local warming in regions currently just south of the Polar Front (e.g. Barker et al., 2009), and through strengthening of the eddy transport of heat across the ACC and enhanced upwelling, causing a more widespread warming of the POOZ. The warming of the Southern Ocean resulted in reduced sea ice which promoted further warming and upwelling (Denton et al., 2010; Xiao et al., 2016; Pedro et al., 2018). There is no palaeo-proxy evidence for eddy transport across the ACC, however modern observations and models show that stronger, southward-shifted SWW cause an increase in eddies (Meredith and Hogg, 2006), leading to an increased poleward heat flux and warmer Southern Ocean temperatures, as well as a southward displacement of the sea ice equilibrium line (Hogg et al., 2007; Screen et al., 2009). During the Younger Dryas the SWW changes may have caused a similar oceanographic response, as both ice cores (Dome Fuji) and marine records support that in the Indian and Atlantic sectors sea ice extent reduced at c.12 ka BP (Bianchi and Gersonde, 2004; Iizuka et al., 2008; Xiao et al., 2016). This would have promoted warming of the lower troposphere and Antarctica by ice-albedo feedbacks (Pedro et al., 2018). Greater upwelling has been shown by higher opal deposition to the south of the Polar Front in the Southern Ocean (Atlantic, Indian and Pacific sectors) through the period 12.7-11.5 ka BP, which has been attributed to increased wind-driven upwelling and a response to the reduction in sea ice extent (Figure 8D; Dezileau et al., 2003; Anderson et al., 2009; Siani et al., 2013). Finally, the combination of greater upwelling and reduced sea ice allowed more outgassing of CO_2 to the atmosphere (Figure 8G), causing warming globally (Monnin et al., 2001; Anderson et al., 2009; Clark et al., 2012; Saunders et al., 2018).

The warming and reduced sea ice shown by the COR1GC reconstructions during the Younger Dryas (Figure 3 and Figure 4) coincides with many of these changes, including the AMOC weakening, strengthened and southward-shifted SWW, increased upwelling, reduced sea ice and rising CO_2 (Figure 8). This sequence of events is also supported by evidence of increased productivity and therefore upwelling on the Conrad Rise, as tentatively inferred from the slightly increased diatom abundances at 12.7-12 ka BP (Figure 8E). Although the marine records have sources of age uncertainty, including potential changes in reservoir ages of 100-200 years (Siani et al., 2013), the similarity in the timing of changes in marine and terrestrial records supports that warming was a result of processes connected with the interhemispheric oceanic and atmospheric reorganisation (Figure 8).

One challenge is to establish the relative importance of each of the outlined causes of warming, because although changes occurred synchronously they may not have all contributed equally to warming of the Southern Ocean. For example,

https://doi.org/10.5194/cp-2020-23
Preprint. Discussion started: 5 March 2020

the Conrad Rise is located close to the modern Polar Front and therefore a southward shift of the SWW during the Younger Dryas may have pushed the Polar Front to the south, leading to warming. Indeed a southward shift is indicated by an increase in Polar Front species at c.12 ka BP (Figure 3). Although observations and models show that the fronts of the Polar Front are topographically constrained in this region (Pollard and Read, 2001; Graham et al., 2012; Pauthenet et al., 2018), it is possible that larger magnitude changes in the SWW were able to divert the Polar Front to the south of the Conrad Rise. Alternatively, the warming shown by the COR1GC reconstruction may have been primarily caused by the rising atmospheric CO_2 levels, which resulted from the above described changes in circulation and Southern Ocean conditions. Principle component analysis on a synthesis of global temperature reconstructions spanning the last deglaciation indicate that temperatures globally were primarily controlled by greenhouse gas concentrations (Clark et al., 2012) and temperature over Antarctica rose synchronously with CO_2 increases during the Younger Dryas (Parrenin et al., 2013). Therefore, given the timing and synchronicity between CO_2 increases and some of the temperature records (COR1GC, MD07-3088 and ice core records) it is possible that CO_2 caused much of the warming and acted as a strong positive feedback mechanism following initial warming and sea ice loss.

5.2.2 Holocene

The warmth during the early Holocene (12-8.7 ka BP) in the southern high latitudes following the Younger Dryas warming has been attributed to high annual, winter and spring insolation levels (Shevenell et al., 2011; Xiao et al., 2016). In the open ocean the insolation may have resulted in enhanced surface warming due to an extended spring-summer season compared to the late Holocene. Alternatively, the strength of the SWW may have influenced the SST. Reconstructions support that the SWW were weaker between 11 and 7 ka BP (Fletcher and Moreno, 2011; Saunders et al., 2018; Figure 8C) and that atmospheric circulation was more meridional (Mayewski et al., 2013), which was potentially caused by the reduced latitudinal insolation and temperature gradient at this time (Divine et al., 2010; Saunders et al., 2018). The more meridional circulation may have led to a greater poleward penetration of warm air masses and therefore warming over the Southern Ocean. However this is uncertain as modern observations instead show that weaker SWW's cause reduced eddy activity and less poleward heat transport across the ACC, resulting in cooling (Hogg et al., 2007; Screen et al., 2009).

At ca. 8.2 ka BP the SiZer analysis indicated that there was a significant cooling in the COR1GC record (Figure 5), while the diatom record by Katsuki et al. (2012) from the Conrad Rise also showed an increase in cold species at 8 ka BP. The duration and timing of the SST cooling observed in the COR1GC record coincides with an AMOC reduction and North Atlantic cooling associated with the 8.2 event (Ellison et al., 2006) however it has not generally been observed in records from the southern hemisphere (Alley and Ágústsdóttir, 2005). Although there are some indications of a cooling in ice core records at this time (Figure 7 E and F; EPICA Community Members, 2006; Jouzel et al., 2007) this spans a longer interval and the few high resolution SST records from the open ocean do not show a cooling (Figure 7; TN057-13PC4; TN057-17TC; Nielsen et al. 2004; Anderson et al., 2009). Therefore although there appears to have been a cooling on the Conrad Rise at this time it

https://doi.org/10.5194/cp-2020-23
Preprint. Discussion started: 5 March 2020


Climate of the Past Discussions

cannot be reliably associated with the 8.2 ka event in the northern hemisphere without additional evidence from other high resolution marine sediment records.

From the mid to late Holocene the high latitude insolation decreased (Divine et al., 2010), causing the SWW's to shift northwards (Lamy et al., 2001), which together can explain the gradual cooling in the COR1GC record (Figure 4). The Spring latitudinal insolation gradient also increased (Divine et al., 2010) causing the SWW's to strengthen (e.g. Saunders et al., 2018), which may have caused cooling by promoting enhanced northward Ekman transport of cooler water from the south towards the Conrad Rise (e.g. Hall and Visbeck, 2002; Lovenduski and Gruber, 2005). The strengthened winds may also have increased upwelling and therefore productivity, however it is not clear if this occurred as although there was a gradual increase in sedimentation rate, potentially reflecting an increased deposition of diatoms (Figure 2), the estimated diatom abundance decreased (Figure 3).

The COR1GC SST record also shows increasingly variable SSTs through the mid to late Holocene after 8 ka BP (Figure 4). Another record from the Conrad Rise found an increased frequency of cold events from 5.5 ka BP onwards (Katsuki et al., 2012) and the closest ice core record, EDML, shows increasing variability in the $\delta^{18}O$ record from c.6 ka BP onwards (EPICA Community Members, 2006; Fischer et al., 2007; Figure 7E). Spectral analysis conducted on the COR1GC SST record identifies significant quasi-periodicities of ~220 to 260 years (Figure 6) during the last 12,000 years. Similar cyclicities of 200-300 years have previously been observed in Southern Ocean paleoceanographic records, including those reflecting SST, sea ice and productivity changes, which were attributed to solar forcing and/or internal climate variability (Leventer et al., 1996; Bárcena et al., 1998; Nielsen et al., 2004; Crosta et al., 2007). Additionally, model simulations have shown a 200-300 year pattern of variability in Southern Ocean temperature that is particularly prominent in the Indian and Atlantic sectors (Latif et al., 2013). These observations and model results support an ocean-atmosphere coupling, as warm (cold) SST's coincide with weakened (strengthened) atmospheric circulation and a negative (positive) SAM (Latif et al., 2013). Although there are no SAM reconstructions spanning the whole Holocene, a record spanning the last 3000 years shows multi-centennial quasi-periodic variations in the SAM index (Moreno et al., 2014) and a 2600 year record of westerly wind intensity from the Falkland Islands has shown a 250 year cycle, linked to solar variability (Turney et al., 2016). The variations in the atmosphere may therefore be linked with the COR1GC SST variability during the mid-late Holocene. The increase in variability in the mid-late Holocene could also be linked with the increasing occurrence of rapid climate change events globally (Mayewski et al., 2004) and the establishment of modern ENSO amplitude and frequency (e.g. Moy et al., 2002), which may have led to greater climate variability over the southern high latitudes.

6 Conclusions

The COR1GC reconstruction of SST variability at the Conrad Rise in the west Indian Sector of the Southern Ocean spans the period from 14.2 to 1 ka BP with an average resolution of ~60 years. SST's were cool (~2.9°C) from 14.2-12.9 ka

https://doi.org/10.5194/cp-2020-23
Preprint. Discussion started: 5 March 2020


Climate of the Past Discussions

BP during the ACR before temperatures increased to 5°C between 12.9 and 11.6 ka BP during the Younger Dryas/Termination 1b. During the Holocene there was a gradual decrease in temperatures; SST's were warmer and stable between 12 and 9 ka BP, before a cooling at c.8.2 ka BP, which was followed by greater SST variability through the period 8-1 ka BP.

The timing and duration of warming in the COR1GC record at 12.9-11.6 ka BP reflects warming also shown by a precisely dated marine record of SST from the Pacific (Siani et al., 2013) and Antarctic ice core temperature records, supporting that atmospheric and ocean temperatures varied in phase. The COR1GC warming also coincides with palaeo-evidence for a weakened AMOC, rising CO_2 levels, greater upwelling in the Atlantic sector of the Southern Ocean, southward displacement and strengthening of the SWW and reduced sea ice, each of which may have contributed to warming in the Southern Ocean. The results support that the warming was initiated by an interhemispheric oceanic and atmospheric reorganisation during the Younger Dryas but does not allow attribution of the relative importance of each process to warming.

For the Holocene period, the most striking change in the COR1GC record is the switch from warm and stable to cooler and variable conditions at 8.7 ka BP, potentially linked with a global reorganisation of the climate system. It is suggested that the early Holocene warmth may have resulted from spring insolation extending the summer season, or as a result of increased poleward transport of heat in the atmosphere as the SWW weakened. During the mid to late Holocene the enhanced variability may represent the establishment of modern coupled atmosphere-ocean relationships outlined in Latif et al. (2013), whereby the SAM and SST's in the Southern Ocean vary in phase over centennial timescales. This is supported by the identification of a quasi-periodic oscillation of ~200-260 years in the Holocene section of the COR1GC SST reconstruction, which mirrors similar centennial variability identified in reconstructions of the SAM and westerly winds.

Code/data availability

The completed dataset can be obtained at pangaea.de

Author Contributions

LCO developed the SST record and wrote the manuscript. XC did data analysis, training and writing/editing of the manuscript. DD did SiZER analysis. AM, DD, KH, EI, RM edited the manuscript. AM, KH, EI, XC, RM conceptualised and supervised the project. LW and OT conducted laboratory analysis. MI provided core material.

Competing interests

The authors declare that they have no conflict of interest.

https://doi.org/10.5194/cp-2020-23
Preprint. Discussion started: 5 March 2020

Acknowledgments

This work was funded by the Research Council of Norway (grant no. 248776/E10) and Ministry of Earth Science, Earth System Science Organization (MoES/Indo-Nor/PS-2/2015), through the OCTEL project. We would like to thank Svetlana Divina and Linda Rossignol-Malaizé for preparation of the foraminifera samples for radiocarbon dating. Gravity core sampling and subsample preparation were partly supported by JSPS KAKENHI (grant no. 23244102, 17H06318). RM would like to thank the Director, NCPOR, India for the support to the project and this is NCPOR Contribution No. XXXX.

References

Alley, R. B. and Ágústsdóttir, A. M.: The 8k event: Cause and consequences of a major Holocene abrupt climate change. Quat. Sci. Rev., 24(10–11), 1123–1149, doi:10.1016/j.quascirev.2004.12.004, 2005.

Anderson, R. F., Ali, S., Bradtmiller, L. I., Nielsen, S. H. H., Fleisher, M. Q., Anderson, B. E. and Burckle, L. H.: Wind-driven upwelling in the southern ocean and the deglacial rise in atmospheric CO_2. Science, 323(5920), 1443–1448, doi:10.1126/science.1167441, 2009.

Anilkumar, N., Luis, A. J., Somayajulu, Y. K., Babu, V. R., Dash, M. K., Pednekar, S. M., Babu, K. N., Sudhakar, M. and Pandey, P. C.: Fronts, water masses and heat content variability in the Western Indian sector of the Southern Ocean during austral summer 2004. J. Mar. Syst., 63(1–2), 20–34, doi:10.1016/j.jmarsys.2006.04.009, 2006.

Ansorge, I. J., Roman, R., Durgadoo, J. V., Ryan, P. G., Dlamini, L., Gebhardt, Z., Rainier, S., Smith, M., Mtonsti and Lutjeharms, J. R. E.: The first oceanographic survey of the Conrad Rise. S. Afr. J. Sci., 104(9–10), 333–336, 2008.

Bárcena, M. A., Gersonde, R., Ledesma, S., Fabrés, J., Calafat, A. M., Canals, M., Sierro, F., J. and Flores, J. A.: Record of Holocene glacial oscillations in Bransfield Basin as revealed by siliceous microfossil assemblages. Antarct. Sci., 10(3), 269–285, doi:10.1017/S0954102098000364, 1998.

Barker, S., Vautravers, M. J., Pike, J., Hall, I. R., Broecker, W. S., Diz, P. and Knorr, G.: Interhemispheric Atlantic seesaw response during the last deglaciation. Nature, 457(7233), 1097–1102, doi:10.1038/nature07770, 2009.

Bendat, J. S. and Piersol, A. G.: Decomposition of wave forces into linear and non-linear components. J. Sound Vib., 106(3), 391–408, doi;10.1016/0022-460X(86)90186-0, 1986.

Berner, K. S., Koç, N. and Godtliebsen, F.: High frequency climate variability of the Norwegian Atlantic current during the early Holocene period and a possible connection to the Gleissberg cycle. Holocene, 20(2), 245–255, doi:10.1177/0959683609350391, 2010.

Bianchi, C. and Gersonde, R.: Climate evolution at the last deglaciation: The role of the Southern Ocean. Earth Planet. Sci. Lett., 228(3–4), 407–424, doi:10.1016/j.epsl.2004.10.003, 2004.

Blaauw, M. and Christen, J. A.: Flexible paleoclimate age-depth models using an autoregressive gamma process. Bayesian Anal., 6(3), 457–474, doi:10.1214/11-BA618, 2011.

https://doi.org/10.5194/cp-2020-23
Preprint. Discussion started: 5 March 2020

Broecker, W. S.: Paleocean circulation during the last deglaciation: a bipolar seesaw? Paleoceanogr., 13(2), 119–121, doi:10.1029/97PA03707, 1998.

Butzin, M., Prange, M. and Lohmann, G.: Radiocarbon simulations for the glacial ocean: the effects of wind stress, Southern Ocean sea ice and Heinrich events. Earth Planet. Sci. Lett., 235(1–2), 45–61, doi:10.1016/j.epsl.2005.03.003, 2005.

Chaudhuri, P. and Marron, J. S.: SiZer for exploration of structures in curves. J. Am. Stat. Assoc., 94(447), 807–823, doi:10.2307/2669996, 1999.

Clark, P. U., Shakun, J. D., Baker, P. A., Bartlein, P. J., Brewer, S., Brook, E., Carlson, A. E., Cheng, H., Kaufman, D. S., Liu, Z., Marchitto, T. M., Mix, A. C., Morrill, C., Otto-Bliesner, B. L., Pahnke, K., Russell, J. M., Whitlock, C., Adkins, J. F., Blois, J. L., Clark, J., Colman, S. M., Curry, W. B., Flower, B. P., He, F., Johnson, T. C., Lynch-Stieglitz, J., Markgraf, V., McManus, J., Mitrovica, J. X., Moreno, P. I. and Williams, J. W.: Global climate evolution during the last deglaciation. Proc. Natl. Acad. Sci., 109(19), E1134–E1142, doi:10.1073/pnas.1116619109, 2012.

Crosta, X., Debret, M., Denis, D., Courty, M. A. and Ther, O.: Holocene long- and short-term climate changes off Adélie Land, East Antarctica. Geochem., Geophys., Geosyst., 8(11), doi:10.1029/2007GC001718, 2007.

Crosta, X. and Koç, N.: Chapter eight diatoms: From micropaleontology to isotope geochemistry. Develop. Mar. Geol., 1, 327–369, doi:10.1016/S1572-5480(07)01013-5, 2007.

Crosta, X., Sturm, A., Armand, L. and Pichon, J. J.: Late Quaternary sea ice history in the Indian sector of the Southern Ocean as recorded by diatom assemblages. Mar. Micropaleontol., 50(3–4), 209–223, doi:10.1016/S0377-8398(03)00072-0, 2004.

Crosta, X., Denis, D. and Ther, O.: Sea ice seasonality during the Holocene, Adélie Land, East Antarctica. Mar. Micropaleontol., 66(3–4), 222–232, doi:10.1016/j.marmicro.2007.10.001, 2008.

Debret, M., Sebag, D., Crosta, X., Massei, N., Petit, J. R., Chapron, E. and Bout-Roumazeilles, V.: Evidence from wavelet analysis for a mid-Holocene transition in global climate forcing. Quat. Sci. Rev., 28(25–26), 2675–2688, doi:10.1016/j.quascirev.2009.06.005, 2009.

Denton, G. H., Anderson, R. F., Toggweiler, J. R., Edwards, R. L., Schaefer, J. M. and Putnam, A. E.: The Last Glacial Termination. Science, 328(5986), 1652 LP-1656, doi:10.1126/science.1184119, 2010.

Dezileau, L., Bareille, G. and Reyss, J. L.: The 231Pa/230Th ratio as a proxy for past changes in opal fluxes in the Indian sector of the Southern Ocean. Mar. Chem., 81(3–4), 105–117, doi:10.1016/S0304-4203(02)00070-1, 2003.

Divine, D. V., Koç, N., Isaksson, E., Nielsen, S., Crosta, X. and Godtliebsen, F.: Holocene Antarctic climate variability from ice and marine sediment cores: Insights on ocean-atmosphere interaction. Quat. Sci. Rev., 29(1–2), 303–312, doi:10.1016/j.quascirev.2009.11.012, 2010.

Ellison, C. R. W., Chapman, M. R. and Hall, I. R.: Surface and deep ocean interactions during the cold climate event 8200 years ago. Science, 312(5782), 1929–1932, doi:10.1126/science.1127213, 2006.

EPICA Community Members: One-to-one coupling of glacial climate variability in Greenland and Antarctica. Nature, 444(7116), 195, doi:10.1038/nature0530, 2006.

https://doi.org/10.5194/cp-2020-23
Preprint. Discussion started: 5 March 2020

Fischer, H., Fundel, F., Ruth, U., Twarloh, B., Wegner, A., Udisti, R., Becagli, S., Castellano, E., Morganti, A., Severi, M., Wolff, E., Littot, G., Röthlisberger, R., Mulvaney, R., Hutterli, M. A., Kaufmann, P., Federer, U., Lambert, F., Bigler, M., Hansson, M., Jonsell, U., de Angelis, M., Boutron, C., Siggaard-Andersen, M.-L., Steffensen, J. P., Barbante, C., Gaspari, V., Gabrielli, P. and Wagenbach,, D.: Reconstruction of millennial changes in dust emission, transport and regional sea ice coverage using the deep EPICA ice cores from the Atlantic and Indian Ocean sector of Antarctica. Earth Planet. Sci. Lett., 260(1–2), 340–354, doi:10.1016/j.epsl.2007.06.014, 2007.

Fletcher, M. S. and Moreno, P. I.: Zonally symmetric changes in the strength and position of the Southern Westerlies drove atmospheric CO_2 variations over the past 14 k.y. Geology, 39(5), 419–422, doi:10.1130/G31807.1, 2011.

Graham, R. M., De Boer, A. M., Heywood, K. J., Chapman, M. R. and Stevens, D. P.: Southern Ocean fronts: Controlled by wind or topography? J. Geophys. Res.: Oceans, 117(C8), doi:10.1029/2012JC007887, 2012.

Guiot, J., de Beaulieu, J. L., Cheddadi, R., David, F., Ponel, P. and Reille, M.: The climate in Western Europe during the last Glacial/Interglacial cycle derived from pollen and insect remains. Palaeogeogr., Palaeoclimatol., Palaeoecol., 103, 73–93, doi:10.1016/0031-0182(93)90053-L, 1993.

Guiot, J. and De Vernal, A.: Is spatial autocorrelation introducing biases in the apparent accuracy of paleoclimatic reconstructions? Quat. Sci. Rev., 30(15–16), 1965–1972, doi:10.1016/j.quascirev.2011.04.022, 2011.

Haddam, N. A., Siani, G., Michel, E., Kaiser, J., Lamy, F., Duchamp-Alphonse, S., Hefter, J., Braconnot, P., Dewilde, F., Isgüder, G., Tisnerat-Laborde, N., Thil, F., Durand, N. and Kissel, C.: Changes in latitudinal sea surface temperature gradients along the Southern Chilean margin since the last glacial. Quat. Sci. Rev., 194, 62–76, doi:10.1016/j.quascirev.2018.06.023, 2018.

Hall, A. and Visbeck, M.: Synchronous Variability in the Southern Hemisphere Atmosphere, Sea Ice, and Ocean Resulting from the Annular Mode. J. Clim., 15(21), 3043–3057, doi:10.1175/1520-0442(2002)015<3043:SVITSH>2.0.CO;2, 2002.

Hammer, Ø., Harper, D. A. T. and Ryan, P. D.: PAST: paleontological statistics software package for education and data analysis. Palaeontologia Electronica, 4(1), 9, 2001.

Hogg, A. M. C., Meredith, M. P., Blundell, J. R. and Wilson, C.: Eddy heat flux in the Southern Ocean: Response to variable wind forcing. J. Clim., 21(4), 608–620, doi:10.1175/2007JCLI1925.1, 2007.

Hughen, K. A., Overpeck, J. T., Peterson, L. C. and Trumbore, S.: Rapid climate changes in the tropical Atlantic region during the last deglaciation. Nature, 380(6569), 51–54, doi:10.1038/380051a0, 1996.

Iizuka, Y., Hondoh, T. and Fujii, Y.: Antarctic sea ice extent during the Holocene reconstructed from inland ice core evidence. J. Geophys. Res.-Atmos., 113(15), 1–8, doi:10.1029/2007JD009326, 2008.

Jouzel, J., Masson-Delmotte, V., Cattani, O., Dreyfus, G., Falourd, S., Hoffmann, G., Minster, B., Nouet, J., Barnola, J. M., Chappellaz, J., Fischer, H., Gallet, J. C., Johnsen, S., Leuenberger, M., Loulergue, L., Luethi, D., Oerter, H., Parrenin, F., Raisbeck, G., Raynaud, D., Schilt, A., Schwander, J., Selmo, E., Souchez, R., Spahni, R., Stauffer, B., Steffensen, J. P., Stenni, B., Stocker, T. F., Tison, J. L., Werner, M. and Wolff, E. W.: Orbital and millennial Antarctic climate variability over the past 800,000 years. Science, 317(5839), 793–796, doi: 10.1126/science.1141038, 2007.

https://doi.org/10.5194/cp-2020-23
Preprint. Discussion started: 5 March 2020

Katsuki, K., Ikehara, M., Yokoyama, Y., Yamane, M. and Khim, B. K.: Holocene migration of oceanic front systems over the Conrad Rise in the Indian Sector of the Southern Ocean. J. Quat. Sci., 27(2), 203–210, doi:10.1002/jqs.1535, 2012.

Lamy, F., Hebbeln, D., Röhl, U. and Wefer, G.: Holocene rainfall variability in southern Chile: a marine record of latitudinal shifts of the Southern Westerlies. Earth Planet. Sci. Lett., 185(3–4), 369–382, doi:10.1016/S0012-821X(00)00381-2, 2001.

Latif, M., Martin, T. and Park, W.: Southern Ocean sector centennial climate variability and recent decadal trends. J. Clim., 26(19), 7767–7782, doi:10.1175/JCLI-D-12-00281.1, 2013.

Leventer, A., Domack, E. W., Ishman, S. E., Brachfeld, S., McClennen, C. E. and Manley, P.: Productivity cycles of 200–300 years in the Antarctic Peninsula region: understanding linkages among the sun, atmosphere, oceans, sea ice, and biota. Geol. Soc. Am. Bulletin, 108(12), 1626–1644, doi:10.1130/0016-7606(1996)108%3C1626:PCOYIT%3E2.3.CO;2, 1996.

Levermann, A., Schewe, J. and Montoya, M.: Lack of bipolar see-saw in response to Southern Ocean wind reduction. Geophys. Res. Lett., 34(April), 1–5, doi:10.1029/2007GL030255, 2007.

Locarnini, R. A., Mishonov, A. V, Antonov, J. I., Boyer, T. P., Garcia, H. E., Baranova, O. K., Zweng, C. R., Paver, J. R., Reagan, D. R., Johnson, D. R., Hamilton, M. and Seidov, D.: World ocean atlas 2013. Volume 1, Temperature. Levitus, Ed., A. Mishonov Technical Ed.; NOAA Atlas NESDIS 73, 40 pp, 2013.

Lovenduski, N. S. and Gruber, N.: Impact of the Southern Annular Mode on Southern Ocean circulation and biology. Geophys, Res, Lett,, 32(11), 1–4, doi:10.1029/2005GL022727, 2005.

Mayewski, P.A., Maasch, K.A., Dixon, D., Sneed, S.B., Oglesby, R., Korotkikh, E., Potocki, M., Grigholm, B., Kreutz, K., Kurbatov, A.V. and Spaulding, N.: West Antarctica's sensitivity to natural and human-forced climate change over the Holocene. J. Quat. Sci., 28(1), 40–48, doi:10.1002/jqs.2593, 2013.

Mayewski, P.A., Rohling, E.E., Stager, J.C., Karlén, W., Maasch, K.A., Meeker, L.D., Meyerson, E.A., Gasse, F., van Kreveld, S., Holmgren, K. and Lee-Thorp, J.: Holocene climate variability. Quat. Res., 62(3), 243–255, doi:10.1016/j.yqres.2004.07.001, 2004.

McManus, J. F., Francois, R., Gherardi, J.-M., Keigwin, L. D. and Brown-Leger, S.: Collapse and rapid resumption of Atlantic meridional circulation linked to deglacial climate changes. Nature, 428(6985), 834, doi:10.1038/nature02494, 2004.

Meredith, M. P. and Hogg, A. M.: Circumpolar response of Southern Ocean eddy activity to a change in the Southern Annular Mode. Geophys. Res. Lett., 33(16), 2–5, doi:10.1029/2006GL026499, 2006.

Monnin, E., Indermühle, A., Dällenbach, A., Flückiger, J., Stauffer, B., Stocker, T. F., Raynaud, D. and Barnola, J.-M.: Atmospheric CO_2 Concentrations over the Last Glacial Termination. Science, 291(5501), 112 LP-114, doi:10.1126/science.291.5501.112, 2001.

Moreno, P. I., Vilanova, I., Villa-Martínez, R., Garreaud, R. D., Rojas, M. and De Pol-Holz, R.: Southern annular mode-like changes in southwestern Patagonia at centennial timescales over the last three millennia. Nat. Commun., 5, doi:10.1038/ncomms5375, 2014.

Moy, C. M., Seltzer, G. O., Rodbell, D. T. and Anderson, D. M.: Variability of El Niño/Southern Oscillation activity at millennial timescales during the Holocene epoch. Nature, 420(6912), 162–165, doi:10.1038/nature01194, 2002.

https://doi.org/10.5194/cp-2020-23
Preprint. Discussion started: 5 March 2020

Nielsen, S. H. H., Koç, N. and Crosta, X.: Holocene climate in the Atlantic sector of the Southern Ocean: Controlled by insolation or oceanic circulation? Geology, 32(4), 317–320, doi:10.1130/G20334.1, 2004.

Orsi, A. H., Whitworth III, T. and Nowlin Jr, W. D.: On the meridional extent and fronts of the Antarctic Circumpolar Current. Deep Sea Res. Part I, 42(5), 641–673, doi:10.1016/0967-0637(95)00021-W, 1995.

Park, Y.: Thermohaline structure of the Antarctic Surface Water/Winter Water in the Indian sector of the Southern Ocean. J. Mar. Syst., 17, 5–23, doi:10.1016/S0924-7963(98)00026-8, 1998.

Parrenin, F., Masson-Delmotte, V., Köhler, P., Raynaud, D., Paillard, D., Schwander, J., Barbante, C., Landais, A., Wegner, A. and Jouzel, J.: Synchronous change of atmospheric CO_2 and Antarctic temperature during the last deglacial warming. Science, 339(6123), 1060–1063, doi: 10.1126/science.1226368, 2013.

Pauthenet, E., Roquet, F., Madec, G., Guinet, C., Hindell, M., McMahon, C. R., Harcourt, R. and Nerini, D.: Seasonal meandering of the Polar Front upstream of the Kerguelen Plateau. Geophys. Res. Lett., 45(18), 9774–9781, doi:10.1029/2018GL079614, 2018.

Pedro, J. B., Jochum, M., Buizert, C., He, F., Barker, S., and Rasmussen, S. O.: Beyond the bipolar seesaw : Toward a process understanding of interhemispheric coupling. Quat. Sci. Rev., 192, 27-46, doi:10.1016/j.quascirev.2018.05.005, 2018.

Pollard, R. T., and Read, J. F.: Circulation pathways and transports of the Southern Ocean in the vicinity of the Southwest Indian Ridge. J. Geophys. Res.: Oceans, 106(C2), 2881–2898, doi:10.1029/2000JC900090, 2001.

Reimer, P. J., Bard, E., Bayliss, A., Beck, J. W., Blackwell, P. G., Ramsey, C. B., Buck, C. E., Cheng, H., Edwards, R. L, Friedrich, M., Grootes, P. M., Guilderson, T. P., Haflidason, H., Hajdas, I., Hatté, C., Heaton, T. J., Hoffmann, D. L., Hogg, A. G., Hughen, K. A., Kaiser, K. F., Kromer, B., Manning, S. W., Niu, M., Reimer, R. W., Richards, D. A., Scott, E. M., Southon, J. R.., Staff, R. A., Turney, C. S. M. and van der Plicht, J.: IntCal13 and Marine13 radiocarbon age calibration curves 0–50,000 years cal BP. Radiocarbon, 55(4), 1869–1887, doi:10.2458/azu_js_rc.55.16947, 2013.

Renssen, H., Goosse, H., Crosta, X., and Roche, D. M.: Early holocene laurentide ice sheet deglaciation causes cooling in the high-latitude southern hemisphere through oceanic teleconnection. Paleoceanography, 25(3), 1–15, doi:10.1029/2009PA001854, 2010.

Saunders, K. M., Roberts, S. J., Perren, B., Butz, C., Sime, L., Davies, S., Van Nieuwenhuyze, W., Grosjean, M. and Hodgson, D. A.: Holocene dynamics of the Southern Hemisphere westerly winds and possible links to CO_2 outgassing. Nat. Geosci., 11, 650–655, doi:10.1038/s41561-018-0186-5, 2018.

Schlitzer, R.: Ocean Data View. Retrieved from http://odv.awi.de, 2014.

Schulz, M. and Mudelsee, M.: REDFIT : estimating red-noise spectra directly from unevenly spaced paleoclimatic time series. Comput. Geosci., 28, 421–426, doi: 10.1016/S0098-3004(01)00044-9, 2002.

Schweitzer, P. N.: Monthly averaged polar sea-ice concentration. U.S. Geological Survey Digital Data Series, Virginia, 1995.

Screen, J. A., Gillett, N. P., Stevens, D. P., Marshall, G. J., and Roscoe, H. K.: The role of eddies in the Southern Ocean temperature response to the Southern Annular Mode. J. Clim., 22(3), 806–818, doi:10.1175/2008JCLI2416.1, 2009.

https://doi.org/10.5194/cp-2020-23
Preprint. Discussion started: 5 March 2020

535 Shevenell, A. E., Ingalls, A. E., Domack, E. W. and Kelly, C.: Holocene Southern Ocean surface temperature variability west of the Antarctic Peninsula. Nature, 470(7333), 250–254, doi:10.1038/nature09751, 2011.

Siani, G., Michel, E., Pol-holz, R. De, Devries, T., Lamy, F., Isguder, G., Dewilde, F. and Lourantou, A.: Carbon isotope records reveal precise timing of enhanced Southern Ocean upwelling during the last deglaciation. Nat. Commun., 4, 2758, doi:10.1038/ncomms3758, 2013.

540 Sokolov, S. and Rintoul, S. R.: Circumpolar structure and distribution of the Antarctic Circumpolar Current fronts: 1. Mean circumpolar paths. J. Geophys. Res.: Oceans, 114(C11), doi:10.1029/2008JC005108, 2009.

Stenni, B., Buiron, D., Frezzotti, M., Albani, S., Barbante, C., Bard, E., Barnola, J. M., Baroni, M., Baumgartner, M., Bonazza, M., Capron, E., Castellano, E., Chappellaz, J., Delmonte, B., Falourd, S., Genoni, L., Iacumin, P., Jouzel, J., Kipfstuhl, S., Landais, A., Lemieux-Dudon, B., Maggi, V., Masson-Delmotte, V., Mazzola, C., Minster, B., Montagnat, M., Mulvaney,

545 R., Narcisi, B., Oerter, H., Parrenin, F., Petit, J. R., Ritz, C., Scarchilli, C., Schilt, A., Schüpbach, S., Schwander, J., Selmo, E., Severi, M., Stocker T. F. and Udisti, R.: Expression of the bipolar see-saw in Antarctic climate records during the last deglaciation. Nat. Geosci., 4(1), 46–49, doi:10.1038/ngeo1026, 2011.

Stocker, T. F. and Johnsen, S. J.: A minimum thermodynamic model for the bipolar seesaw. Paleoceanography, 18(4), doi:10.1029/2003PA000920, 2003.

550 Swart, N. C. and Fyfe, J. C.: Observed and simulated changes in the Southern Hemisphere surface westerly wind-stress. Geophys. Res. Lett., 39(L16711), 6–11, doi:10.1029/2012GL052810, 2012.

Turney, C. S. M., Jones, R. T., Fogwill, C., Hatton, J., Williams, A. N., Hogg, A., Thomas, Z. A., Palmer, J., Mooney, S. and Reimer, R. W.: A 250-year periodicity in Southern Hemisphere westerly winds over the last 2600 years. Clim. Past 2, 189–200, doi:10.5194/cp-12-189-2016, 2016.

555 van Beek, P., Reyss, J.-L., Paterne, M., Gersonde, R., van der Loeff, M. R. and Kuhn, G.: 226Ra in barite: Absolute dating of Holocene Southern Ocean sediments and reconstruction of sea-surface reservoir ages. Geology, 30(8), 731–734, doi:10.1130/0091-7613(2002)030%3C0731:RIBADO%3E2.0.CO;2, 2002.

Verleyen, E., Hodgson, D. A., Sabbe, K., Cremer, H., Emslie, S. D., Gibson, J., Hall, B., Imura, S., Kudoh, S., Marshall, G. J., McMinn, A., Melles, M., Newman, L., Roberts, D., Roberts, S. J., Singh, S. M., Sterken, M., Tavernier, I., Verkulich, S.,

560 Van de Vyver, E., Van Nieuwenhuyze, W., Wagner, B. and Vyverman, W.: Post-glacial regional climate variability along the East Antarctic coastal margin—evidence from shallow marine and coastal terrestrial records. Earth-Sci. Rev., 104(4), 199–212, doi:10.1016/j.earscirev.2010.10.006, 2011.

Xiao, W., Esper, O. and Gersonde, R.: Last Glacial - Holocene climate variability in the Atlantic sector of the Southern Ocean. Quat. Sci. Rev., 135, 115–137, doi:j.quascirev.2016.01.023, 2016.

565

https://doi.org/10.5194/cp-2020-23
Preprint. Discussion started: 5 March 2020

Climate of the Past Discussions
Open Access
EGU

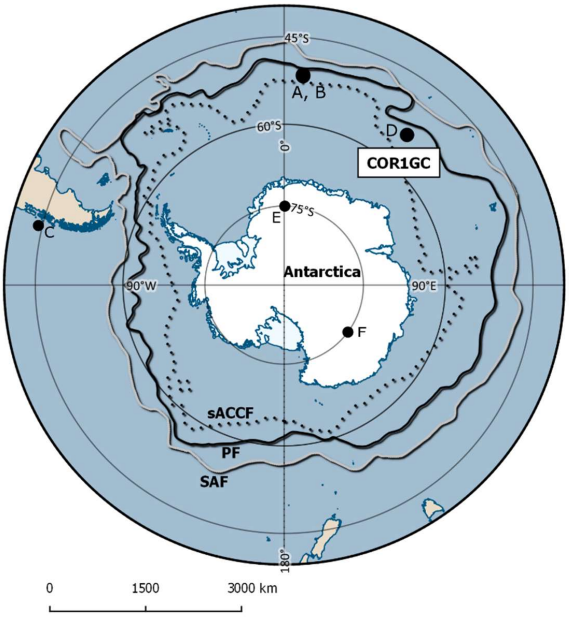

570

Figure 1: Location of core KH-10-7 COR1GC in the western Indian sector of the Southern Ocean. Includes the mean location of the southern Antarctic Circumpolar Current Front (sACCF; dotted line), the Polar Front (PF; black line) and Subantarctic Front (SAF; grey line) according to Orsi et al. (1995). Key terrestrial ice and marine sediment cores mentioned in the text and in Figure 7 are labelled: A) TN057-13-PC4, B) TN057-17-PC1, C) MD07-3088, D) COR1GC, E) EDML, F) EDC.

575

https://doi.org/10.5194/cp-2020-23
Preprint. Discussion started: 5 March 2020

Climate of the Past Discussions
Open Access
EGU

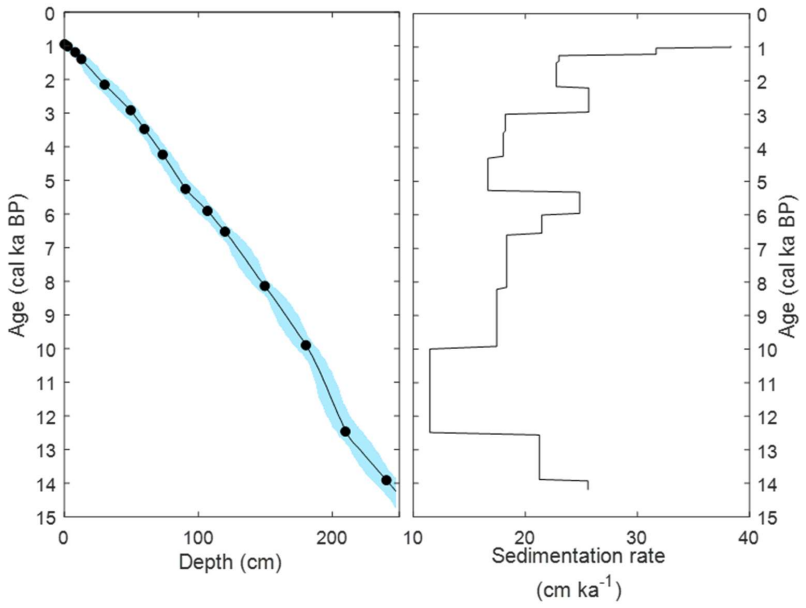

Figure 2: Left: Age-depth model for core KH-10-7 COR1GC. The age model is constrained by 15 calibrated radiocarbon dates, the continuous line is the median age and shaded area represents the 95% confidence interval of the modelled core chronology. Right: Sedimentation rate estimates for COR1GC based on median modelled ages for AMS ^{14}C dates.

580

https://doi.org/10.5194/cp-2020-23
Preprint. Discussion started: 5 March 2020

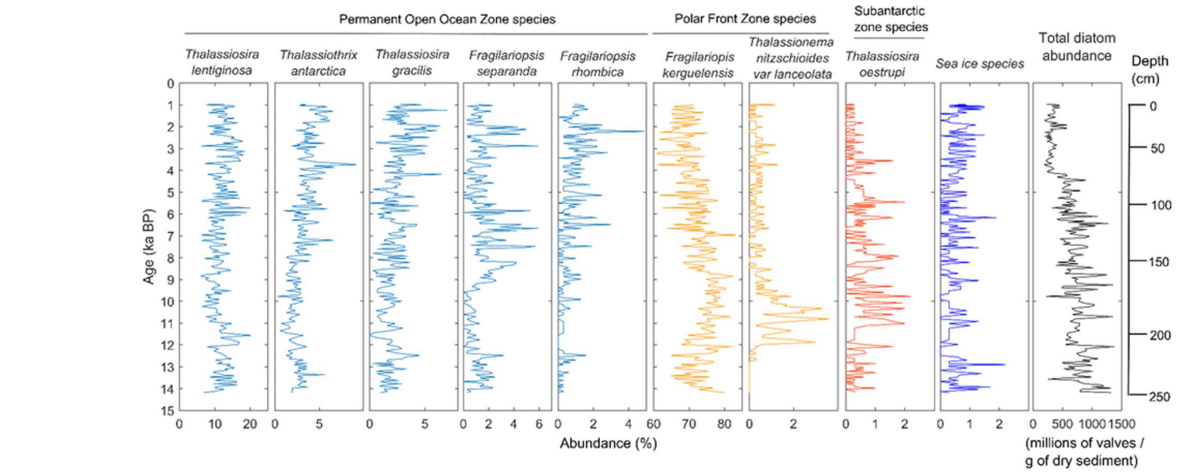

Figure 3: COR1GC diatom abundances as percentages of total sample and the total diatom abundance. Note that the species are plotted on different x-axis scales.

585

https://doi.org/10.5194/cp-2020-23
Preprint. Discussion started: 5 March 2020

Climate of the Past Discussions

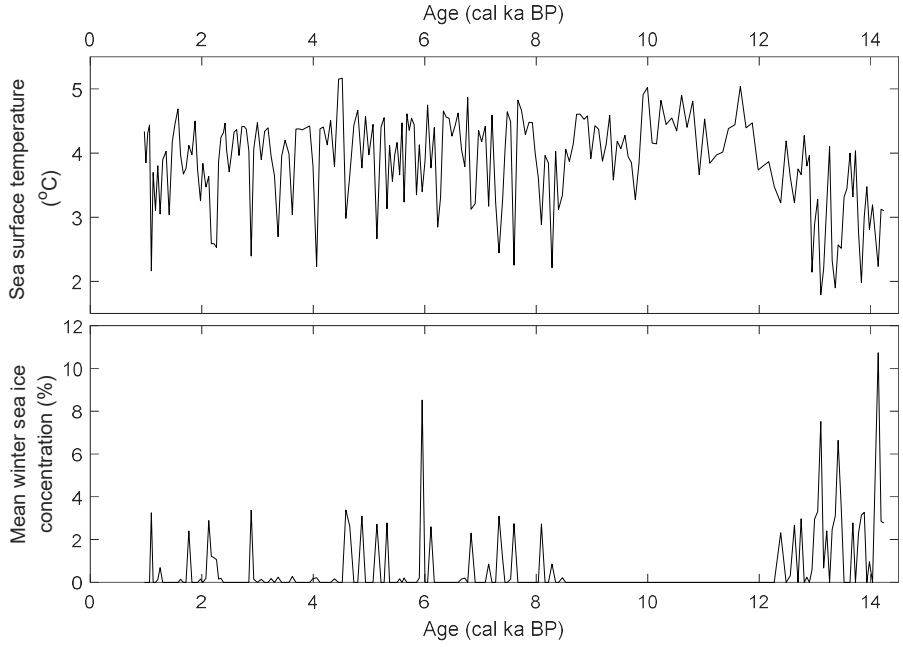

590 **Figure 4: Reconstructed mean summer (January-March) sea surface temperature and mean winter (September) sea ice concentrations for COR1GC.**

https://doi.org/10.5194/cp-2020-23
Preprint. Discussion started: 5 March 2020

Climate of the Past Discussions
Open Access
EGU

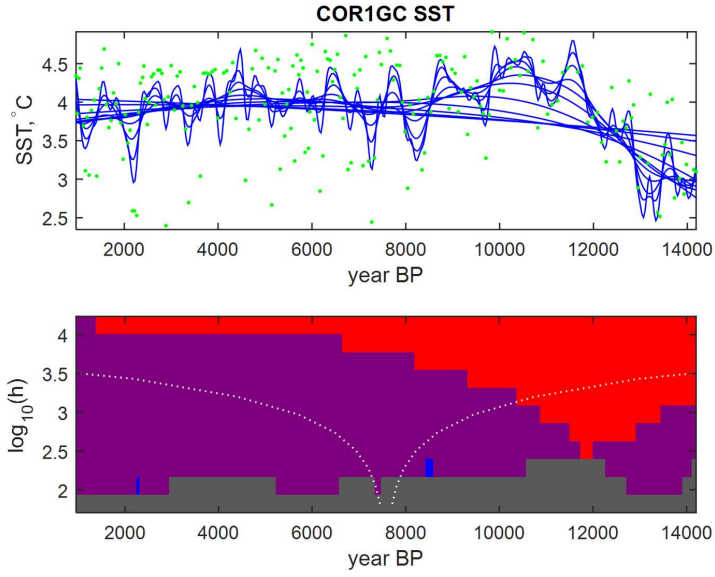

Figure 5: SiZer analysis of the COR1GC SST reconstruction. Upper panel: Family plot of the reconstructed SST. The green dots represent the raw data. Blue lines show the family of smoothings obtained by the local linear kernel estimator for a range of bandwidths (scales h). Bottom panel: A SiZer map, given as a function of location (time t) and scale h. A significantly positive (increased SST) derivative is flagged as red while a significantly negative (decreased SST) derivative is flagged as blue. The color purple is used at locations where the derivative is not significantly different from zero. The color dark gray is used to indicate that too few data points are available to do a correct inference. The distance between the two dotted lines in the cone-shaped curve for a horizontal line in the SiZer plot can be interpreted as the scale for that level of resolution.

https://doi.org/10.5194/cp-2020-23
Preprint. Discussion started: 5 March 2020

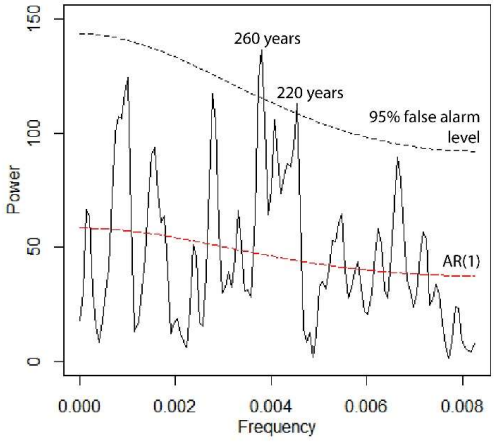

Figure 6: REDFIT spectral analysis of the COR1GC SST reconstruction during the period 12-1 ka BP. The 95% significance level (Chi2) is shown by the dashed black line. The time series is fitted to an AR(1) red noise model (dashed red line).

605

https://doi.org/10.5194/cp-2020-23
Preprint. Discussion started: 5 March 2020

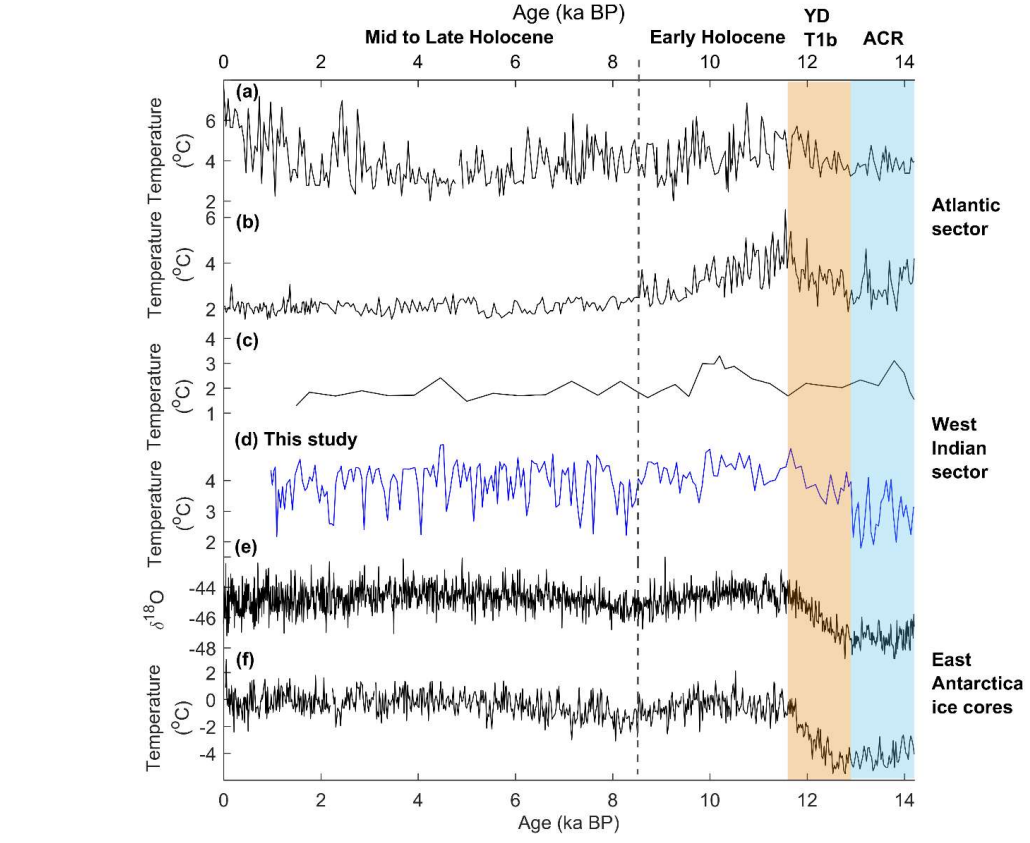

Figure 7: Reconstructions reflecting temperature since 14.2 ka BP from the Southern Ocean and Antarctica at locations shown in Figure 1. A) TN057-17-PC1 diatom-based SST reconstruction (Nielsen et al., 2004), B) TN057-13-PC4 diatom-based SST reconstruction (Anderson et al., 2009), C) PS2606-6 diatom-based SST reconstruction from the Conrad Rise (Xiao et al., 2016), D) COR1GC SST reconstruction (this study) from the Conrad Rise, E) EDML ice core $\delta^{18}O$ reconstruction (EPICA Community Members, 2006), F) EDC ice core temperature reconstruction (Jouzel et al., 2007).

https://doi.org/10.5194/cp-2020-23
Preprint. Discussion started: 5 March 2020

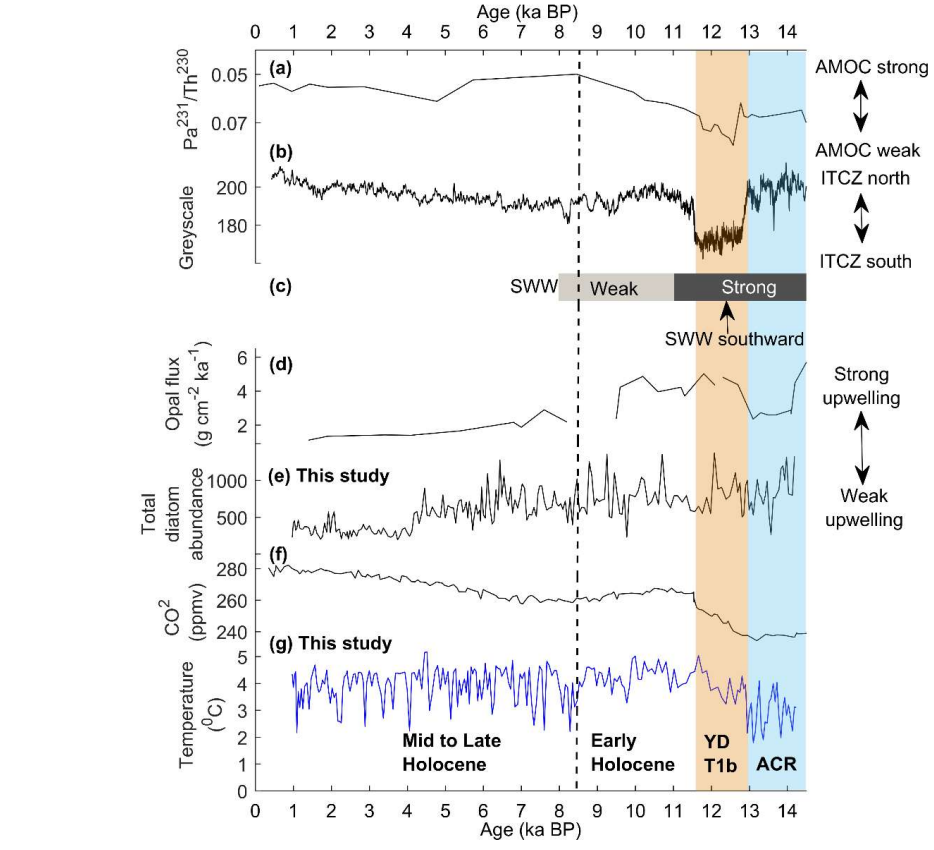

615

Figure 8: Summary of key reconstructions showing the late deglacial to Holocene variations in the AMOC, atmospheric circulation and Southern Ocean. A) AMOC reconstruction based on Pa^{231}/Th^{230} from a core from the western subtropical North Atlantic (McManus et al., 2004); B) greyscale measurements from cores from the Cariaco Basin related to productivity, interpreted as reflecting ITCZ position (Hughen et al., 1996); C) summary of reconstructed SWW strength based on a collation of palaeoclimate
620 **data from the southern mid latitudes (41–52°S; Fletcher and Moreno, 2011); D) upwelling in Atlantic sector of Southern Ocean (core TN057-13PC4) based on opal flux (Anderson et al., 2009); E) productivity at the Conrad Rise inferred from the total diatom abundance in COR1GC, measured in units - millions of diatom valves per gram of dry sediment; F) EDC CO_2 reconstruction (Monnin et al., 2001); G) COR1GC reconstruction of SST (this study).**

625

https://doi.org/10.5194/cp-2020-23
Preprint. Discussion started: 5 March 2020

Climate of the Past Discussions
Open Access
EGU

630 **Table 1: AMS radiocarbon dates and calibrated age estimates.**

Laboratory code	Depth (cm)	^{14}C age (years BP)	Age error (years)	Calibrated median age and 95% confidence age range (calibrated years BP)
ETH-80023/24	0.6	2003	60	970 (770 – 1160)
BETA-485984	2.9	1910	30	1030 (850 – 1200)
BETA-485985	8.6	2040	30	1210 (104 – 1390)
ETH-80025/26	13.2	2370	65	1410 (1210 – 1640)
BETA-488823	30.5	3000	30	2170 (1900 – 2460)
ETH-80027/28	50	3521	65	2930 (2640 – 3280)
BETA-488824	60.2	4070	30	3490 (3200 – 3800)
ETH-80029/30	73.9	4634	70	4250 (3920 – 4640)
BETA-488825	90.9	5480	30	5270 (4900 - 5560)
ETH-80031/60	107.3	5966	70	5930 (5670 – 6230)
BETA-488826	120.4	6580	30	6540 (6290 – 6840)
BETA-488827	150.1	8160	30	8160 (7860 – 8440)
BETA-488828	180.8	9600	40	9920 (9530 – 10350)
BETA-488829	210.3	11570	40	12490 (11740 – 12840)
BETA-488830	240.9	12890	40	13930 (13530 – 14400)